SPACE-TIME-RANGE THREE DIMENSIONAL ADAPTIVE PROCESSING

Shengqi Zhu, Guisheng Liao, Yi Qu, Zhengguang Zhou

(National Lab of Radar Signal Processing, Xidian University, Xi'an 710071, China)

ABSTRACT

Space-time adaptive processing (STAP) is an effective tool for moving target detection. Conventional STAP methodologies process the angular and Doppler two dimensional data vector. In practical applications, adjacent range cells are statistically dependent due to filtering, since the point spreading function of a target is not an ideal delta function. In this paper, a novel approach incorporating range (fast time) information in STAP is presented for clutter rejection, which we term space-time-range adaptive processing (STRAP). This method takes advantage of the correlation information of neighboring range cells. Therefore, the stationary clutter can be suppressed better compared with traditional STAP algorithms ignoring fast time information, resulting in more effective moving target detection. The validity of the STRAP algorithm is verified by the experiments of processing the real measured data of the three-channel X-band radar and MCARM radar systems.

Index Terms**—**Space-time adaptive processing (STAP), Ground moving target indication (GMTI), Synthetic aperture radar (SAR), Doppler beam sharpening (DBS), Space-time-range adaptive processing (STRAP).

1. INTRODUCTION

In airborne radars, due to the motion of the platform, the Doppler shift of the stationary clutter seen by the radar varies with the looking angle, which spreads the Doppler of clutter returns. Since the Doppler band of the clutter masks the moving targets, the detection performance of slowly moving targets is severely degraded. One of the possible solutions is to use the STAP approach. STAP can suppress the clutter effectively and greatly improve the detection performance of the airborne phased array radar [1-2].

The full STAP processor with an exactly known statistic characteristic of the clutter plus interference and noise (i.e., with clairvoyant $\mathbf{R}_{C+J+N}$) is considered as optimum processing for moving target detection. However, the computational load of full-DoF STAP is prohibitive and the large supported samples needed to estimate covariance matrix $\mathbf{R}_{C+J+N}$ can not be obtained in practice. These disadvantages of full-DoF STAP lead to the development of reduced rank and reduced dimension STAP algorithms [3-5]. These approaches have lower complexity and need fewer supported samples compared to the full-DoF STAP algorithm, and have nearly optimum performance. In some practical scenarios, the extreme heterogeneity of the clutter results few training data vectors for the covariance matrix estimation. Algorithms with small auxiliary samples or no training samples have also attracted the attention of many researchers [6-7]. In addition, the modern airborne radar with the synthetic aperture radar (SAR) capability has been proposed recently. STAP combined with multi-channel SAR system has played a very important role in ground moving target indication (GMTI) [8].

Actually, a target after range compression does not occupy only one range cell, which is called the leakage phenomenon. Unlike the traditional STAP algorithms, in this paper, we make full use of the fast time information, and obtain three dimensional data vector (space-time-range) to suppress the non-moving clutter. As a result, the performance of moving targets detection can be improved. The advantages of the proposed algorithm over conventional STAP algorithms can be explained on two aspects as follows:

Case 1: Suboptimum Processing

In suboptimum processing, A multitude of factors contribute to increasing the effective rank of the clutter subspace, such as internal clutter motion (ICM), position array errors, time varying calibration errors, range walk and limited training data samples, etc. Due to the correlation between range CUT and adjacent range cells, the degree of freedom (DoF) of clutter patches increases smaller than that of by STRAP algorithm. Hence, the performance of clutter suppression can be improved.

Case 2: Optimum Processing

In optimum processing, the energy of target can be accumulated if the true spatial temporal range steering vector of the target is constrained exactly. The dimension of noise subspace also increases, just like that in suboptimum processing. The system processor has more DoFs than clutter patches, thus leading to better performance.

2. SIGNAL MOLDELING

Considering the practical situation and the feasibility used in engineering, we combine our approach with reduced dimension STAP schemes such as EFA. Fig. 1 shows the joint data vector formation. Adjacent range cells are utilized to form the joint data vector. Note that the STAP data after Doppler pre-filtering forms an unfocused SAR image, which is named the DBS image. Although the range resolution of the DBS image varies with range cells, adjacent range resolution can be considered as a constant value.

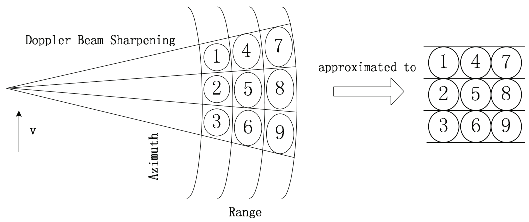

Fig. 1. Relationship between DBS and SAR image pixels.

Fig. 1 shows the relationship between the DBS and SAR image. The statistical properties of range cells are equal to each other approximately. Thus we can join the adjacent range cells to perform adaptive processing.

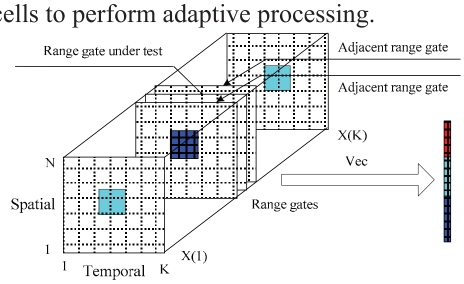

Fig. 2. STRAP data cube and data vector under test.

The joint data vector of the STRAP algorithm is shown in Fig. 2. The data vector involves spatial, temporal and range information. In order to reduce the computational complexity, we can form the data vector with '+' shape, since the point spreading function of the DBS image is '+' shape. What is more, the correlation of pixels selected along the rectangular area lies mainly on that along the '+'shape. The corresponding pixels are shown in Fig. 3. From this figure, we can find the similar data vector in [9] which deals with the estimation of the InSAR interferometric phase. The computational load is equivalent to 5-DoF EFA.

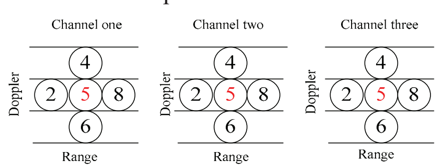

Fig. 3. 3-DoF EFA with three range gates along '+' shape.

Under most circumstances, three Doppler DoFs are sufficient for the EFA algorithm; adding more DoFs does little to improve SINR and complicates training and processing. The input data vector of the 3-DoF EFA can be written as

$$\mathbf{y}(r_n, f_d) = \left[\mathbf{x}^T(r_n, f_{d-1}), \mathbf{x}^T(r_n, f_d), \mathbf{x}^T(r_n, f_{d+1})\right]^T \tag{1}$$

The data of adjacent range gates after Doppler pre-filtering are

$$\mathbf{x}(r_{n-1}, f_d) = \left[x(1, r_{n-1}, f_d), x(2, r_{n-1}, f_d), x(3, r_{n-1}, f_d), \cdots, x(N, r_{n-1}, f_d)\right]^T \tag{2}$$

$$\mathbf{x}(r_{n+1}, f_d) = \left[x(1, r_{n+1}, f_d), x(2, r_{n+1}, f_d), x(3, r_{n+1}, f_d), \cdots, x(N, r_{n+1}, f_d)\right]^T \tag{3}$$

$$\mathbf{y}(r_{n-1}, f_d) = \left[\mathbf{x}^T\left(r_{n-1}, f_{d-\frac{m-1}{2}}\right), \cdots \mathbf{x}^T(r_{n-1}, f_d), \cdots \mathbf{x}^T\left(r_{n-1}, f_{d+\frac{m-1}{2}}\right)\right]^T \tag{4}$$

$$\mathbf{y}(r_{n+1}, f_d) = \left[\mathbf{x}^T\left(r_{n+1}, f_{d-\frac{m-1}{2}}\right), \cdots \mathbf{x}^T(r_{n+1}, f_d), \cdots \mathbf{x}^T\left(r_{n+1}, f_{d+\frac{m-1}{2}}\right)\right]^T \tag{5}$$

The data vector combined with the adjacent range gate is shown as follows:

$$\mathbf{z}(r_n, f_d) = \left[\mathbf{y}^T(r_{n-1}, f_d), \mathbf{y}^T(r_n, f_d), \mathbf{y}^T(r_{n+1}, f_d)\right]^T \tag{6}$$

Thus, the joint spatial temporal range steering vector of the Doppler channel k can be defined as

$$\mathbf{s}_J(\varphi_0, f_d, r_n) = \mathbf{a}(r_n) \otimes \mathbf{a}(f_d) \otimes \mathbf{a}(\varphi_0) \tag{7}$$

$$\mathbf{a}(\varphi_0) = \left[1, e^{j\frac{2\pi d}{\lambda}\cos\varphi_0}, e^{j\frac{4\pi d}{\lambda}\cos\varphi_0}, \cdots, e^{j\frac{2\pi(N-1)d}{\lambda}\cos\varphi_0}\right]^T \tag{8}$$

$$\mathbf{a}(f_d) = \left[g\left(f_{d-\frac{m-1}{2}}\right), \cdots, 1, \cdots g\left(f_{d+\frac{m-1}{2}}\right)\right]^T \tag{9}$$

$$\mathbf{a}(r_n) = \left[g(r_{n-1}), 1, g(r_{n+1})\right]^T \tag{10}$$

$$g\left(f_{d-\frac{m-1}{2}}\right) = \frac{\boldsymbol{w}^H_{d-m-1/2}\boldsymbol{s}(f_d)}{\boldsymbol{w}^H_d\boldsymbol{s}(f_d)} \tag{11}$$

$$g\left(f_{d+\frac{m-1}{2}}\right) = \frac{\boldsymbol{w}^H_{d+m+1/2}\boldsymbol{s}(f_d)}{\boldsymbol{w}^H_d\boldsymbol{s}(f_d)} \tag{12}$$

where $g\left(f_{d-\frac{m-1}{2}}\right)$ and $g\left(f_{d+\frac{m-1}{2}}\right)$ are the beamforming gain of the Doppler channel d on the $-\frac{m-1}{2}$ th and $\frac{m-1}{2}$ th Doppler channels. If we choose the FFT weight as the Doppler channel beamforming weight, $g\left(f_{d-\frac{m-1}{2}}\right)$ and $g\left(f_{d+\frac{m-1}{2}}\right)$ will become zero, since the beamformers of FFT are orthogonal with each other. In most cases, the quiescent weights, such as the chebyshev window, should be added in order to lower the sidelobe level. Then $g\left(f_{d-\frac{m-1}{2}}\right)$ and $g\left(f_{d+\frac{m-1}{2}}\right)$ will be complex values. Just like the Doppler beamforming gain. $g(r_{n-1}) = \frac{\mathbf{w}^H_{r-1}\mathbf{s}_r}{\mathbf{w}^H_r\mathbf{s}_r}$ and $g(r_{n+1}) = \frac{\mathbf{w}^H_{r+1}\mathbf{s}_r}{\mathbf{w}^H_r\mathbf{s}_r}$ are range beamforming gains, where the weight vectors are $\mathbf{w}_r = \left[h_1 s_1, h_2 s_2, \cdots h_L s_L\right]^T$, $\mathbf{w}_{r-1} = \left[\overbrace{h_1 s_1, h_2 s_2 \cdots h_{L-1} s_{L-1}}^{L-1}, 0\right]_L$, $\mathbf{w}_{r+1} = \left[0, \overbrace{h_1 s_1, h_2 s_2 \cdots h_{L-1} s_{L-1}}^{L-1}\right]_L$, and $\mathbf{s}_r = \left[s_1, s_2, \cdots, s_L\right]^T$. $s_1, s_2, \cdots, s_L$ are the samplings of the range matched filter with length L. $\mathbf{w}_r$ is the range matched filtering function of range gate r, and $h_1, h_2, \cdots h_L$ are the quiescent weights, such as the hamming window. In other words, considered an ideal point target at the gate r, the received signal vector $\mathbf{s}_r$ spreads along the range gates. The energy of the target is centralized when compressed with the matched filter function $\mathbf{w}_r$. Hence, $g(r_{n-1})$ and $g(r_{n+1})$ are the normalized compression gains at the adjacent range gates, and are independent on range gates. It is clear that the leaking factors can be determined by the system parameters which are independent on the environment, such as the number of Doppler channels, the number of range gates, the quiescent weights and sampling rates of Doppler channel and range gate. Fig. 4(a) shows the unitary amplitude of the Doppler channel under test and adjacent channels, and 4(b) that of range gate.

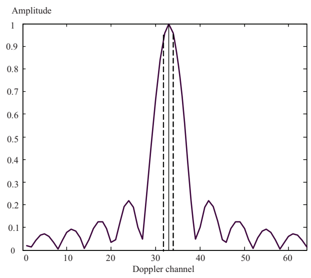

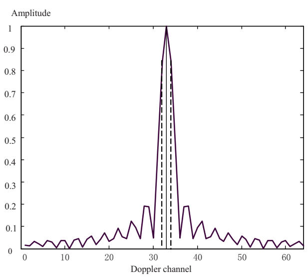

Fig. 4(a). Ideal target Doppler response.

Fig. 4(b). Ideal target range compressed response.

We select range auxiliary channels according to the '+' shape, as shown in Fig. 3. The joint spatial temporal range steering vector is written as

$$\mathbf{s}_J(\varphi_0, f_d, r_n) = \left[\mathbf{s}^T(f_{d-1}), \mathbf{s}^T(f_d), \mathbf{s}^T(f_{d+1})\right]^T \tag{13}$$

where $\mathbf{s}(f_{d-1}) = \mathbf{a}(\varphi_0)$, $\mathbf{s}(f_d) = \mathbf{a}(\varphi_0) \otimes \mathbf{a}(f_d)$, $\mathbf{s}(f_{d+1}) = \mathbf{a}(\varphi_0)$, $\mathbf{a}(\varphi_0) = \left[1, e^{j\frac{2\pi d}{\lambda}\cos\varphi_0}, e^{j\frac{4\pi d}{\lambda}\cos\varphi_0}, \cdots, e^{j\frac{2\pi(N-1)d}{\lambda}\cos\varphi_0}\right]^T$. According to the linearly constrained minimal variance principle [10], the optimum weight of the STRAP algorithm can be written as:

$$\mathbf{w}_J = \frac{\mathbf{R}_J^{-1}\mathbf{s}_J(\varphi_0, f_d, r_n)}{\mathbf{s}_J^H(\varphi_0, f_d, r_n)\mathbf{R}_J^{-1}\mathbf{s}_J(\varphi_0, f_d, r_n)} \tag{14}$$

$$\mathbf{R}_J = \frac{1}{p}\sum_{i=1}^{p}\mathbf{z}(r_i)\mathbf{z}^H(r_i) \tag{15}$$

where $\mathbf{z}(r_i)$ is the joint data vector of the range gate r_i , p is the number of supported samples. These samples should be selected along range gates. According to the Reed Mallett and Brennan rule [11], the number of iid samples must be at least 2q (q is the DoFs of system processor), on the condition that the SNR loss can be controlled to within 3dB.

3. PERFORMANCE ANALYSIS

To carry out the moving targets detection experiment, two types of real raw data with different range resolutions are used. The first experiment is in the SAR mode with a high range resolution of 3.75m. An airborne radar has carried three apertures with the middle aperture transmitting signals and all apertures receiving reflected echoes.

Multichannel Airborne Radar Measurements (MCARM) data set with a low range resolution of 150m is used in the second experiment. The MCARM data and the parameters are listed in [12].

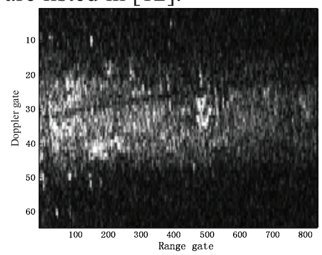

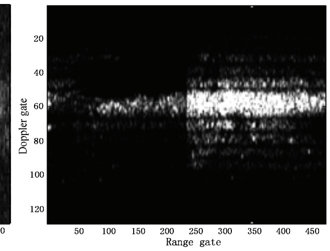

Fig. 5(a). DBS image of scenario one.

Fig. 5(b). DBS image of scenario two.

The DBS images of scenes are shown in Fig. 5(a) and 5(b). In Fig. 5(a), a road orientates mainly in the range direction of the radar on about Doppler channel 30. The main clutter covers about 25 Doppler channels from Doppler channels 20 to 45.

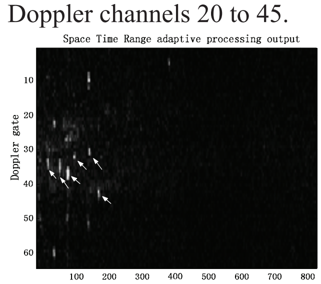

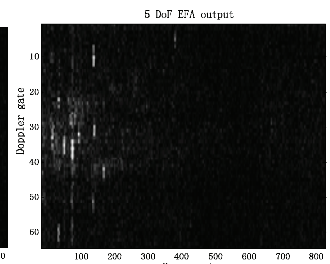

Fig. 6. Detection map of STRAP method.

Fig. 7. Detection map of 5-DoF EFA method.

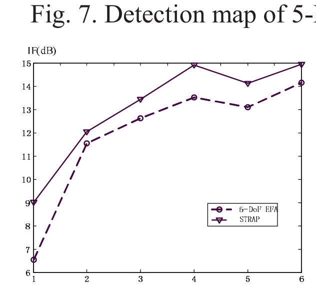

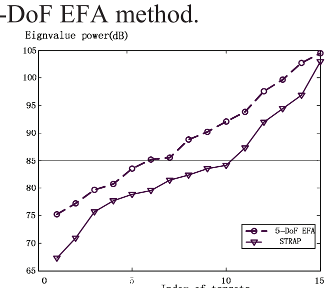

Fig. 8. Improvement factors of moving targets detected.

Fig. 9. Distribution of eigenvalues.

Fig. 6 and 7 show the output of the STRAP and 5-DoF EFA methods, respectively. Training samples are chosen according to the sliding window and are symmetrically selected along the range for CUT. The training scopes are equal for both algorithms. The number of guard cells used is six. Note that the computational loads for both methods are equal. The IF of six moving targets detected is listed in Fig. 8. We can see clearly that, compared with 5-DoF EFA, the IF of moving targets after processing with the STRAP algorithm increases 3dB on average. From Fig. 9, we can also see that the number of the principal eigenvalues by

STRAP algorithm is smaller than that by 5-DoF EFA, thus resulting in better clutter rejection.

To make a good comparison of STRAP and 5-DoF EFA with different velocities, moving targets are injected on Doppler channel 33 along the range bin from 300 to 320 with the radial velocity varying from -8m/s to 8m/s, and also injected on Doppler channel 22 along the range bin from 220 to 240. From Fig. 10, we can see clearly that STRAP is better than 5-DoF EFA in performance. The clutter energy of channel 22 is weaker than that of channel 33, so the maximum value of IF on channel 22 shown in Fig. 11 is lower than that on channel 33 shown in Fig. 10. By the way, the null of IF is not located at the zero radial velocity and the shape of IF is distorted, which is due to the different amplitude and phase errors (array misalignment) on different Doppler channels. Once the phase error is not satisfied with the equation $\triangle\varphi_{31} = 2\triangle\varphi_{21}$, the shape of IF will be distorted.

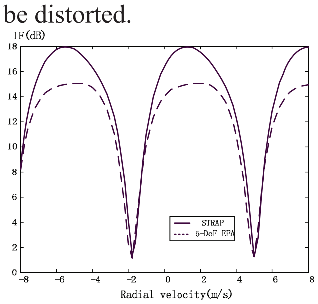

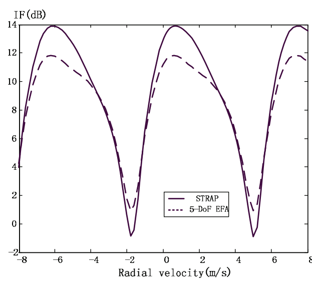

Fig. 10. Statistic IF of Doppler channel 33.
Fig. 11. Statistic IF of Doppler channel 22.

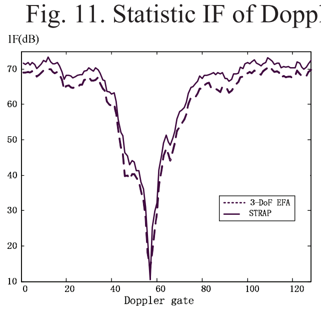

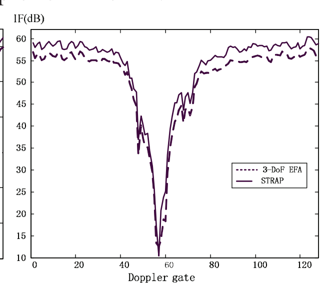

Fig. 12. Statistic IF on strong clutter region.
Fig. 13. Statistic IF on weak clutter region.

In the second experiment with MCARM data, moving targets are injected on Doppler channels from the range bin 350 to 370 where the clutter energy is great and 150 to 170 where the clutter energy is weak. Fig. 12 and 13 show the curves of IF corresponding to great and weak clutter patches, respectively. Under both of the two circumstances, there is an improvement of about 4 dB compared to 3-DoF EFA, which means the target energy leaking to adjacent range cells can be accumulated provided the target steering vector is constrained exactly.

4. CONCLUSIONS

STAP performs excellently on clutter suppression. Like the important role that adjacent Doppler channels play in the post-Doppler STAP (such as EFA) algorithms, the adjacent range cells also are helpful for clutter rejection. In this paper, we join the range CUT with the adjacent range cells to form the joint spatial temporal range data vector. This algorithm is named STRAP. We combine our approach with the reduced-DoF STAP (such as EFA). Adjacent range cells are chosen according to '+' shape, since the point spreading function is '+' shape. The DoFs of the processor increases more than the DoFs of clutter patches. Thus the adaptive processing capability of the processor can be enhanced.

The performance improvement of the STRAP is obvious in practical applications. The key contribution of this paper is the presentation of the STRAP algorithm using the fast time information for clutter rejection. Real measured data processing of two different radar systems verifies the utility and superiority of the proposed STRAP algorithm.

5. REFERENCES

[1] H.S.C.Wang, "Mainlobe clutter cancellation by DPCA for space-Based Radars," *IEEE Aerospace Applications conference*, pp.1-128, Feb. 1991.

[2] R.Klemm, "Introduction to space time adaptive processing," *Electronics &Communication Engineering Journal*, pp.5-12, Feb. 1999.

[3] C.D.Peckham, A.M.Haimovich, J.S.Goldstein, I.S.Reed, "Reduced-Rank STAP Performance Analysis," *IEEE Transactions on Aerospace and Electronic Systems*, pp. 664-676, Apr. 2000.

[4] J.S.Goldstein, I.S.Reed, L.L.Scharf, "A multistage representation of the Wiener filter based on orthogonal projections," *IEEE Transactions on Information Technology*, pp. 2943-2959, 1998.

[5] H.Wang, L.Cai, "On adaptive spatial-temporal processing for airborne surveillance radar system," *IEEE Transactions on Aerospace and Electronic Systems*, pp, 660-670, 1994.

[6] T.K.Sarkar, H.Wang, "A Deterministic Least-Squares Approach to Space-Time Adaptive Processing (STAP)," *IEEE Transactions on Antennas and Propagation*, Jan. 2001.

[7] P.Parker, H.A.Swindle, "Space-Time autoregressive filtering for matched subspace STAP," *IEEE Transactions on Aerospace and Electronic Systems*, pp.510-519, 2003.

[8] J.H.G.Ender, "Space-time processing for multichannel synthetic aperture radar," *Electronics and Communication Engineering Journal*, Feb. 1999.

[9] Z.F.Li, Z.Bao, H.Li, and G.S.Liao, "Image Auto-Coregistration and InSAR Interferogram Estimation Using Joint Subspace Projection," *IEEE Transactions on Geoscience and Remote Sensing*, pp.288-297, 2006.

[10] L.J.Griffiths, C.M.Jim, "An alternative approach to linearly constrained adaptive beamforming," *IEEE Transactions on Antennas and Propagation*, pp. 27-34, 1982.

[11] I.S.Reed, J.D.Mallett, L.E.Brennan, "Rapid convergence rate in adaptive arrays," *IEEE Transactions on Aerospace and Electronic Systems*, pp. 853-863, 1974.

[12] R.D.Brown, R.A.Schneible, M.X.Wicks, H.Wang and Y.Zhang, "STAP for clutter suppression with sum and difference beams," *IEEE Transactions on Aerospace and Electronic Systems*, pp. 634-646, 2000.